

# FLOQUET CONVERGENCE ANALYSIS FOR PERIODIC ACTIVE ROTOR SYSTEMS EQUIPPED WITH TRAILING EDGE FLAPS

J.-B. Maurice<sup>\*</sup>, F.A. King<sup>\*</sup> and W. Fichter<sup>†</sup>,  
University of Stuttgart, Institute of Flight Mechanics and Control, Stuttgart, Germany

<sup>\*</sup>Research assistants (jeanbaptiste.maurice@ifr.uni-stuttgart.de), <sup>†</sup>Professor.  
www.ifr.uni-stuttgart.de

and

O. Dieterich<sup>§</sup> and P. Konstanzer<sup>‡</sup>,  
EUROCOPTER GERMANY GmbH, Dynamics Department, Munich, Germany

<sup>§</sup>Development Engineer, <sup>‡</sup>Manager Dynamics.

## Abstract

Recent technological developments at Eurocopter in the field of actuation based on smart materials allow the secondary control of the rotor blade dynamics directly within the rotating frame by means of piezo-actuated trailing edge flaps. Among many advantages of this technology is the possibility to control different harmonics of the motion of the blade, and thus taking into account the inherent time-periodicity of the rotorcraft. This comes along however with the necessity during controller design phases to prove accurately the stability of the periodic system. In this paper, we highlight the periodic aspect of the considered CAMRAD II helicopter model equipped with trailing edge flaps in comparison to the time-invariant pendant. Floquet stability analysis is performed, rising convergence issues that can lead to false estimation of the plant stability, especially when considering the lowly damped first regressive lagging mode. An example of such deceptive conclusions is presented in the case of a closed-loop system meant to destabilize the first regressive lagging mode using the trailing edge flaps as actuators. The convergence analysis was proved efficient to reestablish trustful Floquet exponents and thus conclude accurately on the stability of the time-periodic system.

## NOMENCLATURE

$T$	=	fundamental period of a linear time-periodic system, s
$\omega_p$	=	pumping or fundamental frequency of a linear time-periodic system, Hz
$\Omega$	=	rotor rotational frequency, Hz
$\mathbf{u}(t)$	=	input signal vector.
$\mathbf{x}(t)$	=	state vector.
$\mathbf{y}(t)$	=	output signal vector.
$t, t_0$	=	time variables, s
$\mathbf{A}(t)$	=	time-periodic state matrix
$\mathbf{B}(t)$	=	time-periodic input matrix
$\mathbf{C}(t)$	=	time-periodic measurement matrix
$\mathbf{D}(t)$	=	time-periodic feedthrough matrix
$\tilde{\mathbf{A}}$	=	time-constant state matrix
$\tilde{\mathbf{B}}$	=	time-constant input matrix
$\tilde{\mathbf{C}}$	=	time-constant measurement matrix
$\tilde{\mathbf{D}}$	=	time-constant feedthrough matrix
$\Phi(t, t_0)$	=	transition matrix from state at $t$ and state at $t_0$
$M_\zeta$	=	blade lagging moments, Nm
$\eta_{TEF}$	=	trailing edge flaps deflection, deg
$[[1, n]]$	=	integers from 1 to $n$

## ABBREVIATIONS

LTI	Linear Time-Invariant
LTP	Linear Time-Periodic
HHC	Higher Harmonic Control
MBC	Multiblade coordinates
TEFs	Trailing Edge Flaps

## 1. INTRODUCTION

Rotorcraft engineers have always been fascinated from the potential of active rotor control allowing the modulation of the lift distribution over the rotor disk beyond the first harmonic. The possibility of shaping the lift distribution over the rotor disk directly affects different disciplines like dynamics (vibration), aero-acoustics (noise) and aerodynamics (performance, fuel consumption, etc). Therefore, the beneficial usage of the additional rotor control degrees of freedom – such as individual blade pitch for blade root actuated systems, trailing edge flap deflections for flap actuated systems or blade twist change for rotor systems with active twist – will lead to significant advantages in the disciplines listed above.

However, the possibility to influence higher harmonics raises the helicopter inherent issue of time-periodicity. In order to properly control such

systems, the control law has to be carefully selected and the design to account for the time-periodic aspect of the plant. In the similar manner the rotor behavior might be improved, it can indeed also be degraded by disadvantageous choice of control. Time-invariant simplification of periodic systems gives satisfying approximations of helicopter rotor models when defined in multiblade coordinates. Though, proving the stability LTP systems remains a necessary drill as performance of control can be for instance reduced because of periodic effect not accounted for.

We propose therefore in this paper to present the analysis, mostly based on the Floquet theory, of a time-periodic helicopter plant. It will be shown that:

- Considering the LTI averaged model only during analysis cannot lead to trustful conclusions on the stability of the plant, even if defined in MBC.
- The number of time-steps over one period contained in the LTP model influences greatly the Floquet value and thus the conclusion on the stability of the system.

After an overview on active rotor systems and linear time-periodic systems, a reliable time-periodic numerical model obtained from the comprehensive helicopter software CAMRAD II [0] and verified by flight test data will be presented. A short theory overview on the Floquet stability analysis will be given. Convergence issues on the stability results will be discussed and a mean to overcome them in order to conclude trustfully on the stability of the system will be proposed.

## 2. ADVANCED ACTIVE ROTOR SYSTEMS

Although the idea of active rotor control has already been introduced into helicopters decades ago starting with higher harmonic actuation of the main rotor swashplate [2,3], advanced active rotor solutions evolved with the availability of piezo-actuated trailing edge flaps which do not affect the primary rotor controls – and thus the safety of the helicopter – in case of potential malfunctions. The related research activities culminated in the world's first flight of a helicopter with active trailing edge flaps in 2005 – a BK117 derivative developed and operated by Eurocopter, see Fig. 1.

Successful open and closed-loop flight tests of this system were performed in different disciplines e.g. in the field of vibration reduction [4]. A detailed description of several design issues for the active rotor of the BK117 is given in [5]. The high interest in the rotorcraft community in such kind of active rotor systems is also documented in a similar full scale system based on a MD900 main rotor and equipped with trailing edge flaps which has recently been tested in the large NASA Ames wind tunnel [6].

Nevertheless, the exploration of the full potential of active rotor systems needs not only adequate

progress in the hardware world but also in the software world asking for advanced control schemes and techniques. A typical approach applied at the beginning of HHC was to perform main control tasks in the frequency domain taking into account the limited capabilities of the hardware at that time i.e. low sampling rates e.g. compared to blade passage frequencies.

In the meantime, progress in control hardware allows performing control tasks also in the time domain with high sampling rates of 1 kHz and beyond. The underlying mechatronic systems enable the engineers to apply modern and complex control theories to active rotor systems such as  $\mathcal{H}_\infty$  synthesis [7] featuring a high number of controller states. Nevertheless – for full exploration of the active rotor system potential – adequate plant models in the time domain are required for model based control approaches.



Fig. 1: Experimental system equipped with piezo-actuated trailing edges (© Eurocopter)

## 3. LINEAR TIME-PERIODIC ASPECT OF HELICOPTERS

Neglecting the tail rotor for a conventional helicopter configuration, the system composed of main rotor and fuselage is typically described by a time periodic system of equations. The time periodicity is evoked by the superposition of the forward flight speed of the entire vehicle plus the main rotor rotation speed leading to velocity asymmetries on advancing and retreating side of the

rotor. Thus, the time-periodicity is introduced into the motion equations of the helicopter and its subsystems by azimuth-dependent aerodynamic loads.

To account for these properties particular to rotorcraft, the helicopter plant dynamics can be generally written as linear time-periodic system ( $L$ ) of order  $n$  with  $m$  inputs and  $p$  outputs as follows

$$(1) \quad (L): \forall t \in [0, T], \begin{cases} \dot{\mathbf{x}}(t) = \mathbf{A}(t)\mathbf{x}(t) + \mathbf{B}(t)\mathbf{u}(t) \\ \mathbf{y}(t) = \mathbf{C}(t)\mathbf{x}(t) + \mathbf{D}(t)\mathbf{u}(t) \end{cases}$$

where  $\mathbf{x}(t) \in \mathbb{R}^n$  is the state vector,  $\mathbf{u}(t) \in \mathbb{R}^m$  the input vector,  $\mathbf{y}(t) \in \mathbb{R}^p$ ,  $\mathbf{A}(t) \in \mathbb{R}^{n \times n}$  the state matrix,  $\mathbf{B}(t) \in \mathbb{R}^{n \times m}$  the input matrix,  $\mathbf{C}(t) \in \mathbb{R}^{p \times n}$  the measurement matrix, and  $\mathbf{D}(t) \in \mathbb{R}^{p \times m}$  the feedthrough matrix of the system.

The periodicity of the matrices yields the properties:

$$(2) \quad \forall t \in [0, T], \begin{cases} \mathbf{A}(t+T) = \mathbf{A}(t) \\ \mathbf{B}(t+T) = \mathbf{B}(t) \\ \mathbf{C}(t+T) = \mathbf{C}(t) \\ \mathbf{D}(t+T) = \mathbf{D}(t) \end{cases}$$

where the fundamental period  $T$  of this system corresponds to the fundamental frequency  $\omega_p = 1/T$ , commonly known also as pumping frequency.

For the application of conventional control theories based on time-invariant systems, it is preferable to modify this system of equations into a time-invariant pendant ( $\tilde{L}$ ):

$$(3) \quad (\tilde{L}): \forall t, \begin{cases} \dot{\mathbf{x}}(t) = \tilde{\mathbf{A}}\mathbf{x}(t) + \tilde{\mathbf{B}}\mathbf{u}(t) \\ \mathbf{y}(t) = \tilde{\mathbf{C}}\mathbf{x}(t) + \tilde{\mathbf{D}}\mathbf{u}(t) \end{cases}$$

Nevertheless, any transformation of time periodic systems to time invariant ones is leading to an approximation for arbitrary systems as information is lost. In the rotorcraft community this approach is widely applied using multiblade transformations and coordinates before averaging the system matrices with respect to the rotor azimuth. The introduction of multiblade coordinates preserve some contributions of time periodicity mapping it into spatial directions related to the cyclic multiblade coordinates.

Comparing the response of linear time invariant systems with linear time periodic systems, it can be demonstrated that harmonic inputs and outputs of time invariant systems are related to the same single frequency while a single harmonic input into a time periodic system can lead to multi-harmonic outputs at different frequencies. Thus, controller concepts based only on linear time-invariant systems do not fully exploit the plant properties for control purposes,

see also [8].

An example is the usage of 2/rev input for vibration control of a four bladed rotor system. The 2/rev input acts on time periodic properties of the plant which e.g. can be seen in the dependency of 2/rev control authority versus flight speed. In hover – assuming approximately axial symmetry and thus no system periodicity – no control authority is available for hub load control based on 2/rev while it is possible for high flight speeds with high system periodicity. Averaging of the matrices for a linear time-invariant system leads to a loss of controllability of the hub loads for 2/rev input.

Nevertheless, in order to exploit the time periodic character of the plant for control purposes, adequate time-periodic models are required based either on numerical models using a model based approach or on models identified by tests.

## 4. NUMERICAL MODEL

### 4.1. Active Rotor Equipped with TEFs

The experimental system on which the numerical model is based is composed of a BK117 airframe serving as test bed and of a hingeless main rotor system of type Boelkow featuring blades which originally evolved from the prototype blades of the EC145, see [9]. The advanced planform of the blades shows inboard tapering and a swept back parabolic tip, see Fig. 2. The rotor has a diameter of 11m and an equivalent chord of 0.325m. Although the aerodynamic layout is kept unchanged compared to the prototype blade, the structural dynamic characteristics are significantly modified due to the integration of the trailing edge flap modules and due to different blade tuning which is e.g. highlighted by a very low blade torsion frequency. The blades offer three different locations in spanwise direction for the insertion of the trailing edge flap modules. The baseline configuration places two active flap modules at the inboard and mid position while the outboard position is occupied by a dummy module. Thus, the trailing edge flap system of the ADASYS rotor is characterized by the key figures of Table 1:

**Table 1:** Blade and trailing edge flaps dimensions

Chord	0.05 m, 15 %
Max. length	0.90 m, 0.16R
Radius station	3.8 - 4.9m
Unit 1	3.95 m, 0.718R
Unit 2	4.25 m, 0.773R
Unit 3	4.55 m, 0.827R
Max. flap angle	$\pm 10$ deg

The TEFs are controlled by piezo actuators featuring one pair of actuators per module. This technology offers advantages in the case of loss of power supply due to the inherent stiffness of the piezo actuators and in view of high actuator bandwidth. Due to the flexibility of the piezo stacks and other elements of the flap modules, the resulting deflection of the trailing edge flaps depends not only on the control input but also on aerodynamic and inertia flap hinge moments which have to be adequately taken into account for modeling purposes.



**Fig. 2:** ADASYS rotor blade featuring active trailing edge flaps

#### 4.2. CAMRAD II Numerical Models

Similar to the hardware, the aeroelastic rotor model of the ADASYS rotor originates from the prototype blade model as well using the comprehensive rotor code CAMRAD II [10]. The structural dynamic description of the blades is modified in order to account for the design changes e.g. required for the installation of the trailing edges. The implementation of the trailing edge flaps lead to a partial re-design of the rotor blade at the radial positions of the trailing edge flaps. Special cut-offs had to be considered during the design process in order to allow the installation of the actuation modules. These cut-offs have an impact on local stiffness and inertia data as well.

Regarding the modeling of the trailing edge flaps the applied rotor code CAMRAD II offers the

possibility to consider them as rigid bodies attached to the flexible rotor blade by hinges. It is important to note that the aeroelastic model incorporates the TEFs not only as aerodynamic devices but also as structural dynamic components with dynamic degrees of freedom in order to adequately account for trailing edge flap control flexibility. Thus, the commanded trailing edge flap deflection might differ from the actual trailing edge deflection due to aerodynamic and inertia loading. The locations of the hinges are defined by three coordinates in radial, chordwise and normal direction of the rotor blades. For the definition of the TEF rigid bodies, flap mass, flap centre of gravity and flap moment of inertia about the hinge axes are required. In order to assign flexibility and damping of the flap actuator, the implementation of hinge spring and hinge damper providing stiffness and viscous damping are typical means in multibody codes. In the current model actuator dynamics are neglected and only actuator flexibility is accounted for. This approach is in line with the high natural frequencies observed by testing.

In view of aerodynamic modeling, the airfoil tables used for the application of lifting line theory within CAMRAD II had to be extended in order to include the trailing edge deflection angle. The aerodynamic layout of the rotor blade is based on airfoils of the last generation of the OA series from the French research organization ONERA. For the table look-up approach of the CAMRAD II rotor code, the aerodynamic coefficients of the airfoils are compiled in table form depending on angle of attack and Mach number. For application of TEFs, these tables have to be extended by an additional dimension – the TEF angle – for those airfoil sections which are affected by the implementation of the flaps. For the extension of the airfoil tables, thin airfoil theory built the theoretical and numerical backbone as at the time of the model set-up only limited CFD results were available. Due to the consideration of linearized airfoil theory, it exists restrictions for Mach numbers, angles of attack and flap deflection angles. For the implementation of the Mach number dependency, compressibility effects of the derivatives are considered according to the Prandtl-Glauert rule up to a Mach number of 0.75. Regarding angles of attack and flap deflection angles, the theory is related to attached flow conditions which matches also the design point for the operation of the trailing edge flaps thus not posing a severe limitation in application.

Fig. 3 shows a fan diagram of the ADASYS rotor in a hover case (i.e. axisymmetrical conditions) presenting the blade mode frequencies of interest for active control purposes.

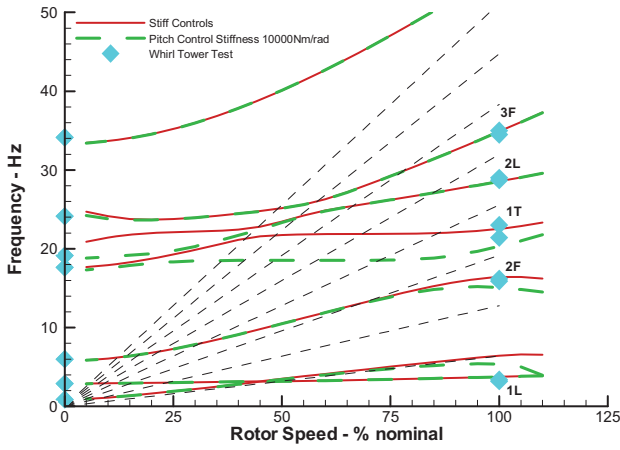


Fig. 3: Fan diagram of the ADASYS rotor.

The special dynamic layout of the ADASYS rotor is reflected by a low fundamental torsion frequency and a pronounced coupling of the torsion mode with the second flap mode in the vicinity of the nominal rotor speed. This behavior is also visible in Fig. 4 showing the gain of the pitch link loads in hover case versus actuation frequency. High gains are noted in the vicinity of the fundamental torsion frequency confirming the special role of the fundamental torsion mode with respect to active rotor control using trailing edge flaps. More information on the aeroelastic issues of the ADASYS rotor can be found in [5].

In this paper, the forward flight at 100kts ( $\mu = 0.23$ ) is retained for the model along the analysis.

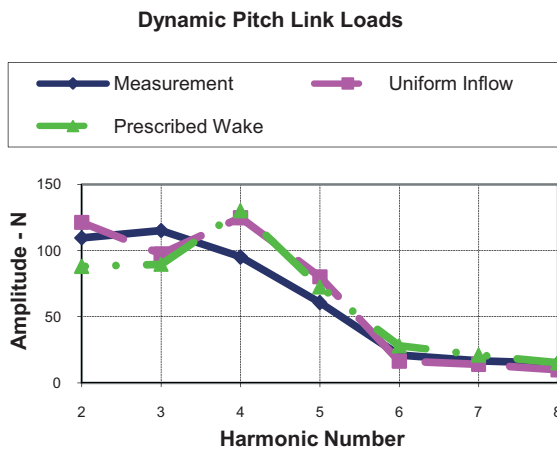


Fig. 4: Dynamic pitch link loads due to flap excitation.

The motion of the blades is described using the five first dynamic modes: 1<sup>st</sup> lagging, 1<sup>st</sup> and 2<sup>nd</sup> flapping, 1<sup>st</sup> torsion and 2<sup>nd</sup> lagging modes defined in multiblade coordinates.

The helicopter airframe body modes, as well as the inflow modes, are in this case not taken into

account for simplicity purposes. The model corresponds therefore to an isolated rotor. It results in a dynamic order  $n = 40$  for the LTP model defined in multiblade coordinates. The state vector can therefore be written as:

$$(4) \quad \mathbf{x} = \begin{bmatrix} \dot{x}_0^1, \dots, \dot{x}_0^5, & \dot{x}_c^1, \dots, \dot{x}_c^5, & \dot{x}_s^1, \dots, \dot{x}_s^5, & \dot{x}_d^1, \dots, \dot{x}_d^5, \\ x_0^1, \dots, x_0^5, & x_c^1, \dots, x_c^5, & x_s^1, \dots, x_s^5, & x_d^1, \dots, x_d^5 \end{bmatrix}^t$$

where the upper index represent the number of the mode\*, and the lower one the coordinate†. The structure of the resulting system matrix can therefore be represented as bloc matrices with:

- $\mathbf{I}_{20} \in \mathbb{R}^{20 \times 20}$ , a diagonal unity matrix.
- $\mathbf{A}_{11}(t) \in \mathbb{R}^{20 \times 20}$  and  $\mathbf{A}_{12}(t) \in \mathbb{R}^{20 \times 20}$ , containing the coupling between the states and their derivatives, and thus the information on the dynamics of the system.
- $\mathbf{O}_{20} \in \mathbb{R}^{20 \times 20}$ , the zero matrix of order 20.

The original matrix can be rewritten in blocs as:

$$(5) \quad \mathbf{A}(t) = \left( \begin{array}{c|c} \mathbf{A}_{11}(t) & \mathbf{A}_{12}(t) \\ \hline \mathbf{I}_{20} & \mathbf{O}_{20} \end{array} \right)$$

### 4.3. Time Averaging and Loss of Information

As for every periodic signal, the elements of the state matrix can be expanded in term of Fourier series in order to reach the harmonic components contained in the periodic signals.

In Fig. 5 to Fig. 7, the different harmonics of the elements of the dynamic matrix  $\mathbf{A}(t)$  are illustrated in order to observe coupling occurring in the different harmonics. For each element, the Fourier expansion is build and the  $m$ -th coefficient of the this expansion is placed in the matrix  $\mathbf{A}_m$ .

It is important to notice that the considered model is defined in multiblade coordinates, so that its pumping frequency is  $\omega_{p,MBC} = 2 \Omega$  as demonstrated in Ref. [1, 11].

\* 1 for first lagging, 2 for first flapping, 3 for second flapping, 4 for first torsion and 5 for second lagging modes.

† 0 for collective, c for longitudinal cyclic, s for lateral cyclic and d for differential.

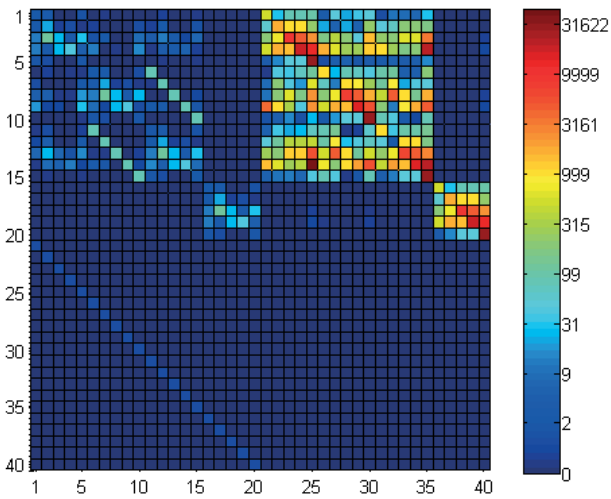


Fig. 5:  $A_0$ , 0-th harmonic of the state matrix.

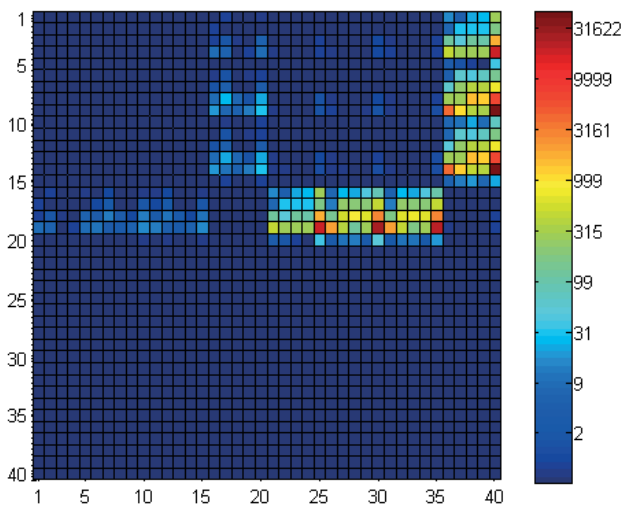


Fig. 6:  $A_1$ , 1<sup>st</sup> harmonic of the state matrix.

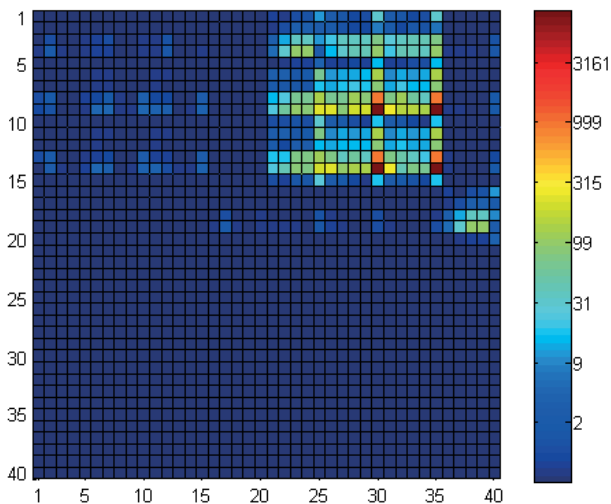


Fig. 7:  $A_2$ , 2<sup>nd</sup> harmonic of the state matrix.

The coupling of the collective and cyclic coordinates to the differential coordinate is absent of the zeroth harmonic, and corresponds to the LTI

averaged matrix.

This coupling is restored when the 1<sup>st</sup> harmonic and higher are taken into account, re- building the time-periodic representation of the helicopter in term of Fourier series.

This phenomenon was also observed in [8] in which the lead-lag moment response of the rotor blade to an impulse on the collective coordinate leads to almost no response on the differential coordinate for the LTI representation.

In Fig. 8, the lead-lag moments' response of the system to an initial disturbance of the first differential lagging mode results in significant couplings of the cyclic coordinates for the LTP system, whereas negligible for the LTI one. The definition of the equations of motion in multiblade coordinates before averaging moderates the loss of information as this spatial transformation restores some small part of the time dependency and thus couplings. Nevertheless, the loss of information is obvious and confirms the fact that only minor coupling is retained using the MBC transformation.

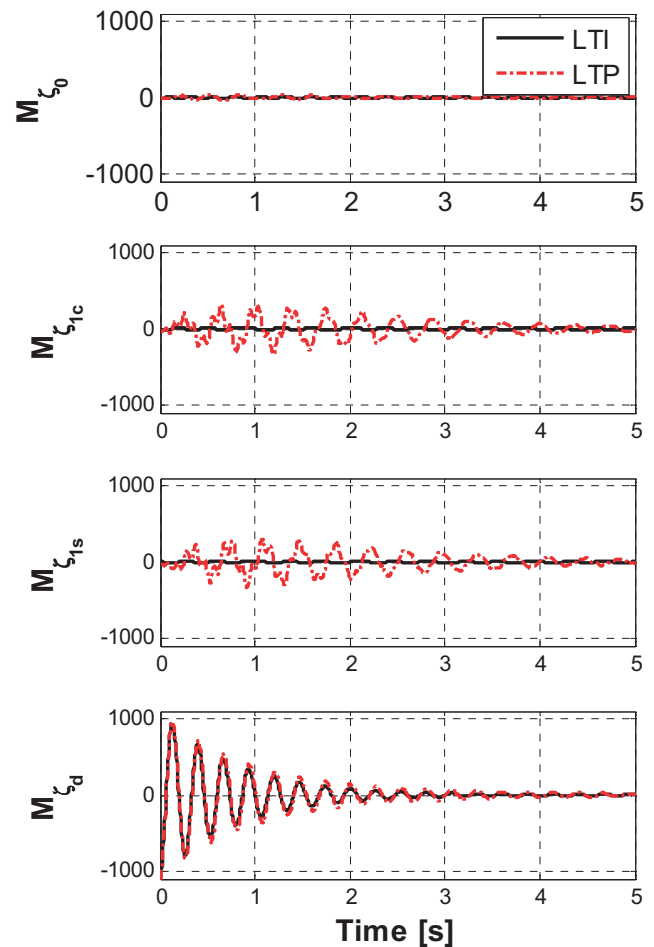
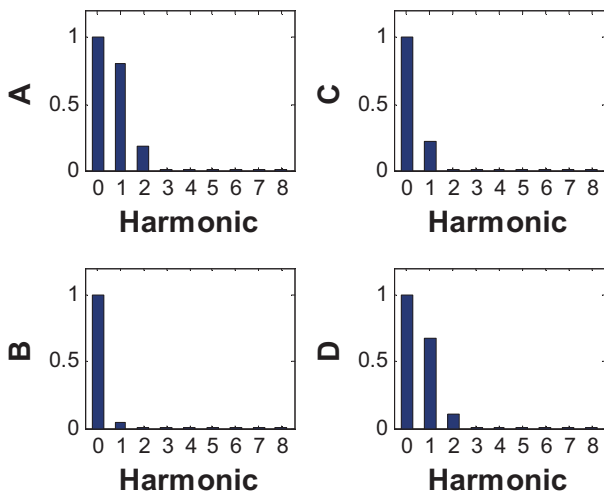


Fig. 8: Time-response of the model to an initial perturbation of the first differential lagging mode.



**Fig. 9:** Frobenius norm of the helicopter model matrices, all are normed to 1.

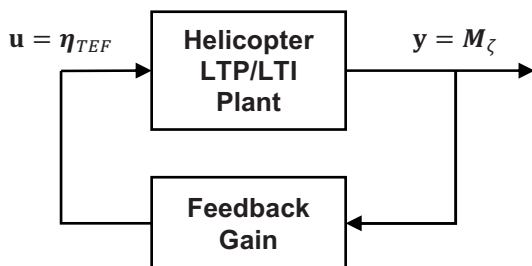
The time dependency of the system is not negligible, so that any controller design for which stability is a sensitive aspect shall be checked by means adapted to the analysis of time-periodic systems.

Fig. 9 provides an overview of the time dependency of the system matrices in term of matrix norm up to the 8-th harmonic. The Frobenius norm (see Appendix) of the Fourier expanded matrices are computed and normed to unity to somehow give a measure of the quantity of information included in each harmonic.

Neglecting harmonics above the second harmonic in the periodic system matrices is foreseen to give a good approximation of the LTP system.

### 5. LTP SYSTEMS AND CONTROLLER DESIGN

We considered the simple closed-loop system of Fig. 11 that aims at destabilizing the rotor system. Inputs are the TEFs deflections  $\eta_{TEF}$ . The blade lagging moments  $M_\zeta$  are fed back with a gain designed to displace the poles of the poorly damped first lagging mode to the limit of stability. The plant



**Fig. 11:** Elementary closed-loop feedback structure destabilizing the lowly damped first lagging mode for the LTP or LTI models.

consists in the numerical model ( $L$ ) and ( $\tilde{L}$ ) presented in the previous part. The LTI model is computed from the LTP one retaining the zeroth harmonic of the system matrices only.

We compute the root locus of the LTI system in closed-loop for an increasing gain (Fig. 10) in order to bring the poles of the first lagging mode near to the imaginary axis. An adequate gain is retained and the LTP and LTI closed-loop systems are used to compute the time-response simulation to an initial first regressive lagging mode disturbance of Fig. 12. The response of the LTI system is as expected stable. On the other hand, the LTP system response is diverging slowly indicating instability that could not be foreseen analyzing the LTI system stability only. This illustrates also the importance of considering LTP system as well during controller design, as a disadvantageous choice can lead to unexpected results when applied straightforward to the time-periodic helicopter plant.

To avoid such unpleasantness, the analysis of the stability of the periodic system in closed-loop shall be performed.

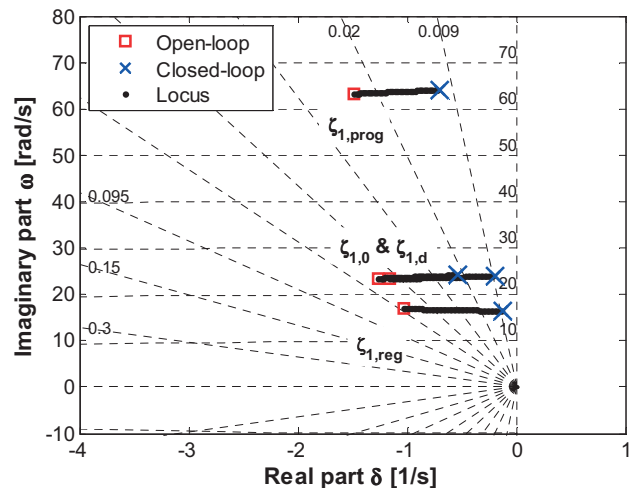


**Fig. 10:** Root locus of the destabilized closed-loop system.

### 6. FLOQUET STABILITY ANALYSIS

The Floquet analysis [12] is used in the case of dynamic systems whose matrices are time-periodic. This well known and very powerful method is particularly adapted to investigate the stability of time-periodic plants, e.g. the helicopter rotor that is  $2\pi$ -periodic. Further details can be found in Mohler [13] for general time-periodic systems. Application to a helicopter plant is extensively presented by Johnson [14].

Valuable contributions on the optimization of run time based on the consideration of the symmetry of the rotor blade done by Peters et al. [15, 16] with the

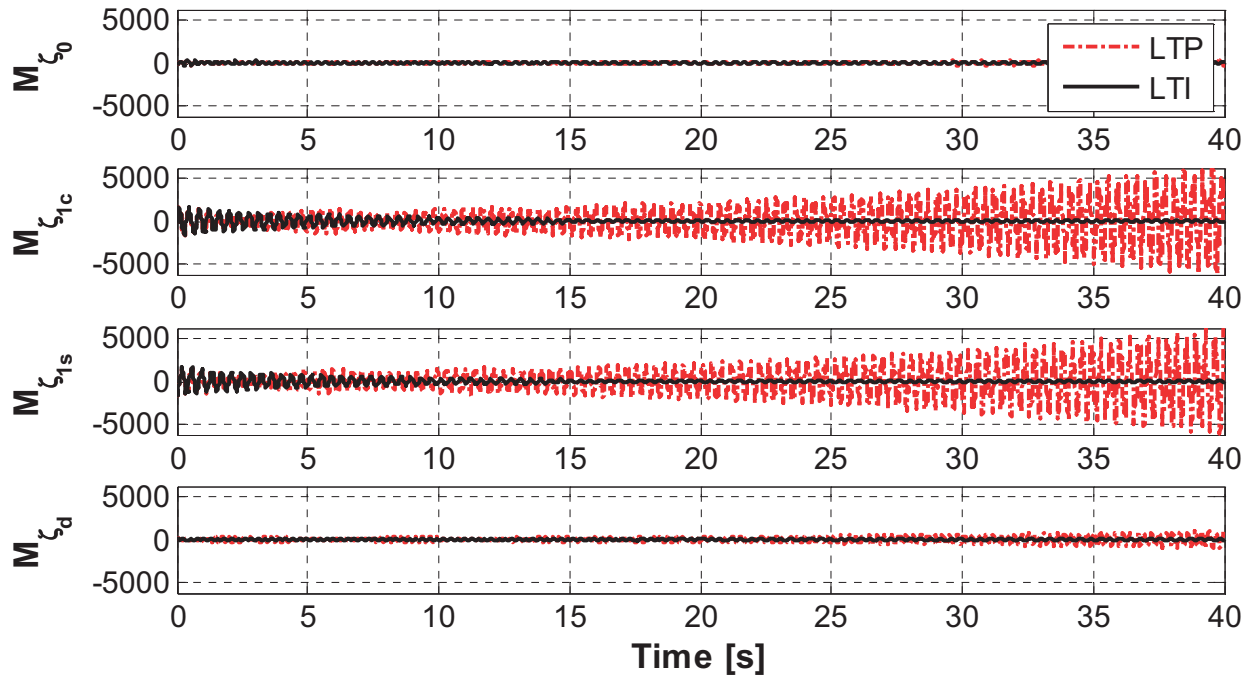


**Fig. 12:** Time-response of the closed-loop LTI and LTP systems to an initial first regressive lagging mode disturbance, forward flight at 100kts

concept of Fast-Floquet theory. Considering the  $Q$ -planes of symmetry of the rotor<sup>‡</sup>, a reduction of computer time by a factor  $Q$  can be achieved in comparison to the classical Floquet approach. Subramanian et al. [17] and Venkataratnam et al. [18] also considered parallel computing to reduce run time. All these techniques aim at reducing the computer time because of formidable run time necessary to compute models of order over 100.

In the case of interest<sup>§</sup> however, and because of progress in computing capacities, run time does not constitute a limitation. To give indications, the most critical computation realized that will be presented later in this paper was run within the minute. The choice of the well known classical Floquet theory was therefore made in this paper.

The theoretical background for the calculation of the Floquet exponents will be depicted in the next section.

### 6.1. Algorithm for the Calculation of the Floquet Exponents

A brief overview of the classical Floquet theory [12] for stability analysis is given in Appendix. In practice [15], the monodromy matrix  $\Phi(T, 0)$  needs to be calculated. Its eigenvalues are the Floquet values that can conclude on the stability of the LTP system.

As the monodromy matrix relates the state at  $t$  to the state at  $t_0$ , the homogeneous equation

$\dot{\mathbf{x}}(t) = \mathbf{A}(t)\mathbf{x}(t)$  of the periodic system can be rewritten:

$$(6) \quad \forall t, t_0, \dot{\Phi}(t, t_0) = \mathbf{A}(t)\Phi(t, t_0)$$

The matrix  $\Phi(T, 0)$  can be calculated by integrating  $\dot{\Phi}(t, 0) = \mathbf{A}(t)\Phi(t, 0)$  over one period. Wang et al. [19] illustrates a numerical method to this purpose<sup>\*\*</sup>. The monodromy matrix is calculated by integrating Eq. (8) over one period. The  $i$ -th column of  $\Phi(T, 0)$  corresponds to the resolution of Eq. (8) using as initial condition  $\mathbf{x}(0)$  the  $i$ -th column of the identity matrix  $\mathbf{I}$ . This calculation therefore needs to be operated  $n$  time if  $n$  is the order of  $\mathbf{A}(t)$ . The algorithm to conclude on the stability of the system using the classical Floquet theory follows logically:

**Listing 1:** Algorithm for the stability analysis by means of Floquet Analysis.

#### a) Calculation of $\Phi(T, 0)$

Integration of  $\dot{\mathbf{x}}(t) = \mathbf{A}(t)\mathbf{x}(t)$  to provide the columns of  $\Phi(T, 0)$ . In mathematical form:

$$\Phi(T, 0) = (\mathbf{x}_1^t, \dots, \mathbf{x}_n^t)$$

where  $\forall i \in \llbracket 1, n \rrbracket$ ,

<sup>‡</sup> This approach applies therefore only to even-bladed rotors.

<sup>§</sup> The considered model has an order 40.

<sup>\*\*</sup>This method is based on the assumption that the differential equation has a minor time dependency. Using the same method for differential equations with a great time dependency could result in serious convergence issues, and is investigated specifically for the helicopter plant in this paper.

$x_i$  solution of the equation  $\dot{\mathbf{x}}(t) = \mathbf{A}(t)\mathbf{x}(t)$   
with initial condition  $\mathbf{x}_i^t(t=0) = (0, \dots, 0, \underset{i}{1}, 0, \dots, 0)$

#### b) Eigenvalues

Calculation of the eigenvalues  $(\theta_i)_{i \in \llbracket 1, n \rrbracket}$  of  $\Phi(T, 0)$

#### c) Conclusion

Is the system asymptotically stable?  $\forall i \in \llbracket 1, n \rrbracket$ ,  $|\theta_i| < 1$ ?

The decisive point is the integration of the homogenous equation  $\dot{\mathbf{x}}(t) = \mathbf{A}(t)\mathbf{x}(t)$ . In the case of models generated by CAMRAD II, the matrix  $\mathbf{A}(t)$  is time-discrete. The model is discretized in  $N$  azimuth steps over one period and indexed with  $k \in \llbracket 1, N \rrbracket$  such that  $\mathbf{A}_k = \mathbf{A}(k\Delta t)$  corresponds to the matrix at the azimuth step  $k\Delta t$ , where the time-step is  $\Delta t = T/N$ .

Different methods exist for the integration. Wang et al. [19] proposes the use of a second-order Runge-Kutta (RK2) scheme for the  $i$ -th column of  $\Phi(T, 0)$ . Because of possible convergence issues related to the importance of time-periodicity in the models, the use of the classical 4-th order Runge-Kutta (RK4) integration scheme is foreseen to give better results:

Both schemes have been implanted in C-MeX functions of MATLAB to ensure low run times<sup>††</sup>. There are benchmarked later on in this paper to conclude on convergence issues.

## 6.2. Verification of Numerical Code

A simple example presented in Van der Kloet et al. [20] is considered as a reference for the testing of the algorithm. The maximal numerical error observed in the calculations when comparing the results from the numerical code and the analytical solution for the eigenvalues in the s-plane was  $\varepsilon = 0,0064$  and therefore validated the integration scheme.

However, Wang et al. [19] showed that the time step for the integration plays a great role in the precision and convergence of the algorithm. In the case of the helicopter model, time-step requirements could be more demanding than for the basic example. These issues are investigated using a complex helicopter model in the next section.

## 7. CONVERGENCE ISSUES

Floquet theory is based on the fact, that the information of the behavior of a LTP system is fully contained in one period. Using Floquet theory means looking at the system as if it is discretized in

time steps equal to the system period.

There exists a unique map from each state within a period to the same state after one period. The eigenvalues of these maps are alike, and they are the Floquet exponents. But like in digital control, a sampling only makes sense if the sampling rate fits the dynamics that are to be captured. This is a parallel to the Floquet theory. Problems with the Floquet theory will occur when the pumping frequency of the system is much greater or smaller than the frequencies of the internal dynamics<sup>††</sup>:

- If the pumping frequency is much greater than the frequencies of internal dynamics, they are well captured by the Floquet exponents. Again drawing the parallel to sample data systems this corresponds to a high sampling rate. On the other hand, the calculation of the Floquet exponents from one period is more complex because of the high amount of data. The convergence of the algorithm worsens and the calculations necessitate high integration time step.
- If the pumping frequency is much smaller than the frequencies of the internal dynamics, all Floquet exponents of a stable system will lie close to zero in the z-plane.

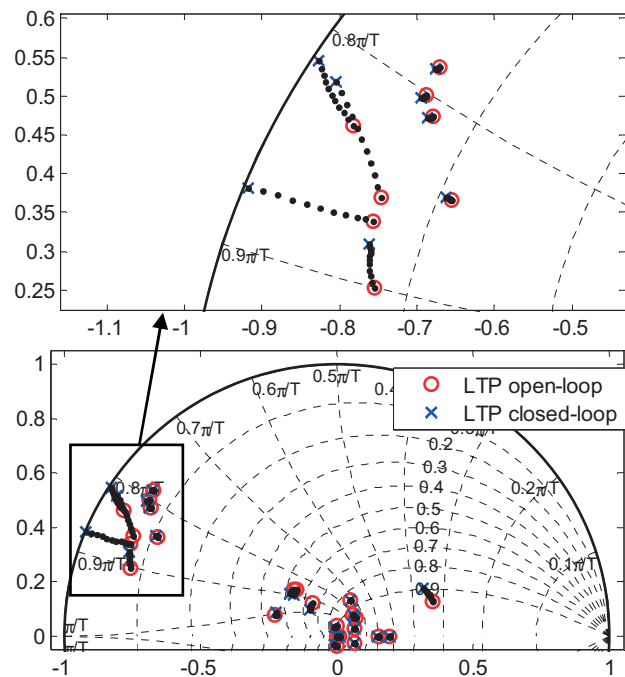


**Fig. 13** Root locus of Floquet exponents of the destabilized LTP system with 100 steps/rev.

<sup>††</sup> The implementation of the code in C-Mex MATLAB function reduced the run time by a factor 10.

<sup>††</sup> There is an additional problem defining frequencies for internal dynamics, as the definition common to LTI theory is not applicable to LTP systems. The frequencies of the internal dynamics have to be calculated from a system response in order to be properly detected.

Only in the case when the frequencies of the internal dynamics have a similar order of magnitude compared to the system period Floquet theory can provide the illustrative results desired. The Floquet exponents will have to be checked for convergence in the case of the helicopter rotor model, which has modes with frequency below and above the pumping frequency.

As for every method based on the integration of discrete system, the time-step is foreseen to be the cause of the deficiency.

### 7.1. Interpolation of Models

As we could only obtain models in CAMRAD II with up to 100 steps per revolution, a way shall be found to obtain a much more precise decomposition of the system over one period<sup>§§</sup>. To overcome this difficulty, the matrices of the models are interpolated linearly element-wise to augment the number of steps per revolution. This corresponds to an upsampling. This method shall be tested though as it could lead to unreliable results.

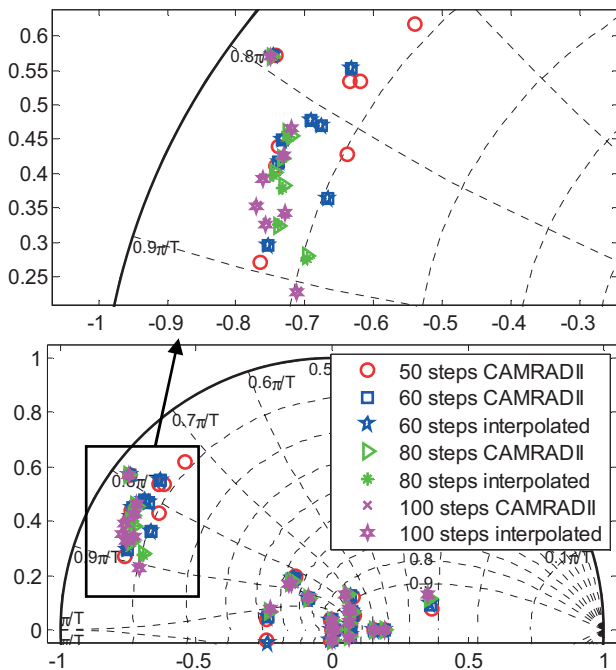


**Fig. 14:** Comparison of the Floquet exponents for interpolated and directly computed CAMRAD II LTP models. The integration scheme is RK4.

To this purpose, models with 50, 60, 80 and 100 steps/rev have been computed directly in CAMRAD II. Using a 50 steps/rev discretized model as baseline, the other models are interpolated using upsampling rate of 1.2, 1.6 and 2.0 obtaining thus the models with 60, 80 and 100 steps respectively.

<sup>§§</sup> This corresponds to a diminution of the time step, or an upsampling of the data.

The possibility to use the Fourier harmonic components  $A_m$  of the periodic matrix  $A(t)$  to restore the time series with an increased number of steps has been also considered. The choice of linear interpolation has nevertheless been made as this simple method gives satisfactory results.

Fig. 14 presents the comparison of the Floquet exponents in open-loop calculated from CAMRAD II models and interpolated models. Different observations can be made. Only a residual error can be observed between the values of the Floquet exponents of interpolated models and the originals ones: The interpolation method is considered as valid in this paper for the use on CAMRAD II helicopter rotorblade.

The influence of the number of integration steps is obvious as the exponents move with an increasing number of steps. When situated near the stability limit  $|\theta_i| < 1$ , the exponents undergo this influence more intensively. The close-up of Fig. 14 presents an example of such strongly influenced exponents. They correspond in this case to the lowly damped first and second blade lagging modes.

### 7.2. Convergence of Floquet Exponents

The analysis is pursued further augmenting significantly the number of discrete matrices representing the LTP helicopter system over one period in order to investigate the convergence of the Floquet exponent's calculation, especially with respect to those lowly damped lagging modes.

In Fig. 15, the number of steps per revolution is increased with linear interpolation from 100 steps/rev up to 10000 steps/rev. The RK4 integration scheme is used to compute the monodromy matrix. The motion of the Floquet exponents is obvious for low number of steps/rev and decelerates when the number of steps/rev increases strongly indicating convergence.

To investigate the convergence, the norm of the exponents obtained with the RK2 and RK4 integration scheme are plotted in Fig. 16 with an increasing number of steps. As expected, for a low number of steps/rev, in the domain where the convergence index varies strongly, the RK4 method produces more reliable results than the RK2 one. The computation is considered as convergent above 500 steps/rev.

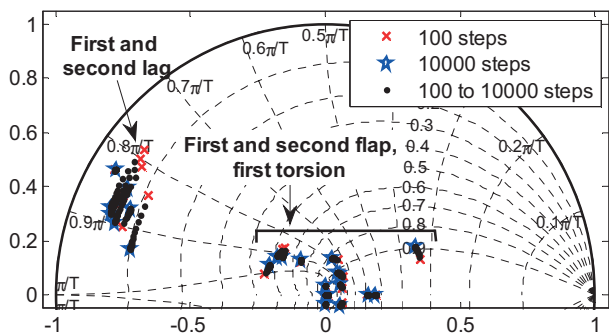


Fig. 15: Floquet exponents of the open-loop system for an increasing number of steps/rev. The integration scheme is RK4.

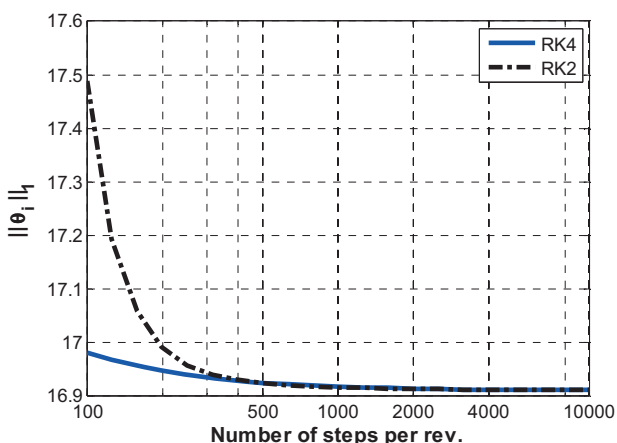


Fig. 16: Norm of the vector of Floquet exponents for an increasing number of steps/rev, comparison of the RK2 and RK4 integration schemes.

8. BENEFIT OF THE PRESENTED ANALYSIS

The results observed in the convergence analysis are taken into account for the stability investigations of the LTP system in closed-loop.

The locus of the Floquet exponents of Fig. 13 is reconsidered not only for an integration using 100 steps/rev that was proven to have a insufficient time-steps, but this time with a discretization up to 10000 steps/rev.

The Floquet exponent corresponding to the first regressive lagging mode is clearly influenced by the number of steps/rev used for the calculation of the transition matrix (close-up in Fig. 17), and moreover crosses the stability border when the number of steps is increased consequently. This effect has a major impact on the conclusions concerning the stability of the system. This also restores trustful results that could not be obtained with insufficient number of steps/rev.

Going further we reduced slightly the gain of the feedback structure. The locus of Floquet exponents is build and convergence analysis is performed

concluding that the system is stable. This is confirmed by the time-response of Fig. 19.

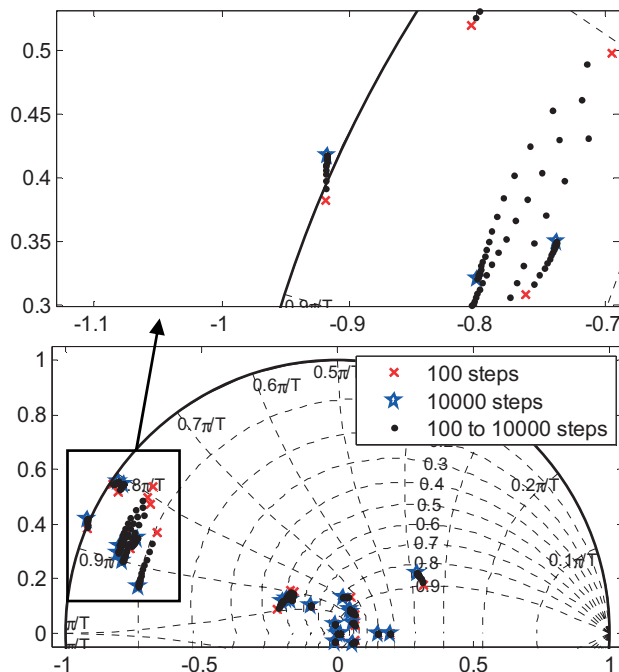


Fig. 17: Locus of the Floquet exponents of the closed-loop system for an increasing number of steps/rev. The integration scheme is RK4.

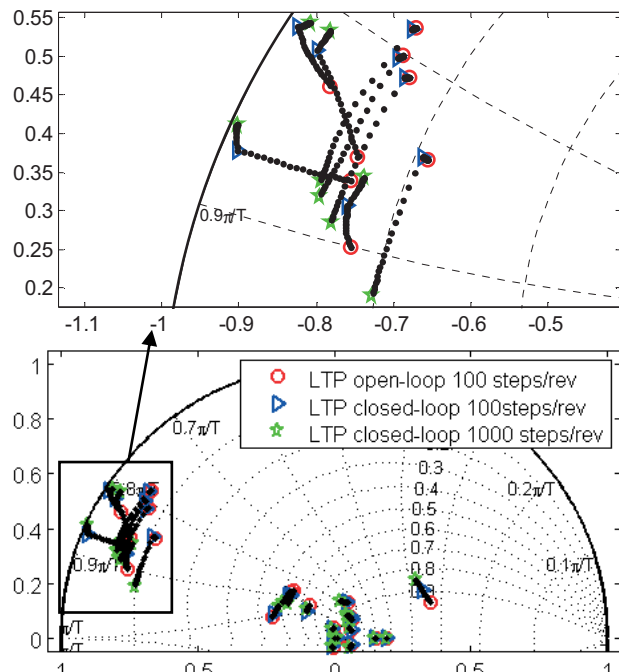
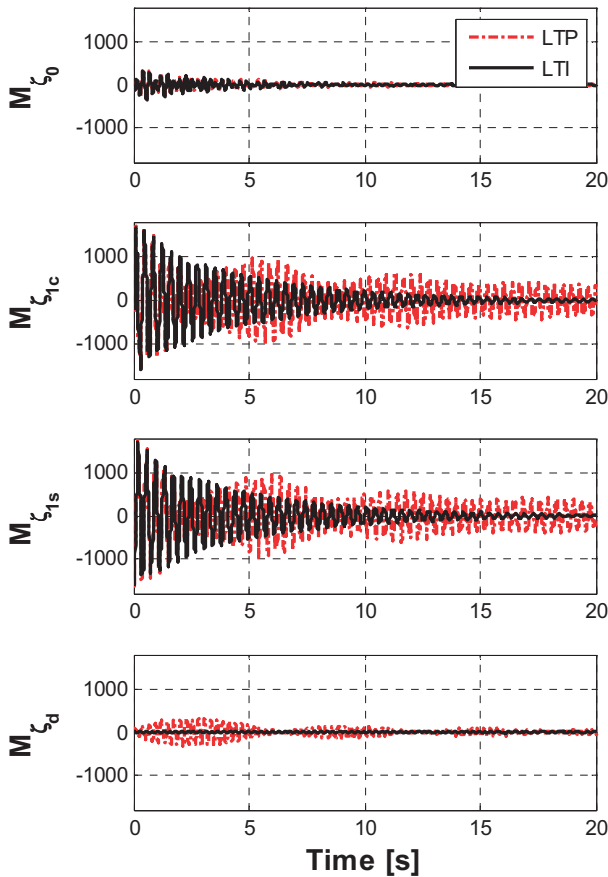


Fig. 18: Locus of the Floquet exponents of the closed-loop system with a reduced gain compared to Fig. 10 and Fig. 17. This case is ensured to be stable.



**Fig. 19:** Time-response of the stable closed-loop LTI and LTP systems. Stability was ensured with convergence study on the precision of the Floquet exponents.

## CONCLUSIONS

We presented in this paper the analysis of a time-periodic helicopter model based on the Eurocopter demonstrator equipped with active trailing edge flaps. This model has been tested and verified during different flight campaign and constitute a reliable system plant. The analysis of the harmonics of LTP system confirms that important information is lost when the system is averaged resulting in a time-invariant pendant of the original plant and neglecting interconnections occurring in higher harmonics.

Neglecting this periodic information means in most of cases no arm with respect to stability if, for instance during a controller design, sufficient phase reserve is planned to overcome the uncertainty induced by the suppression of higher harmonics. However the analysis using Floquet theory provides a straightforward mean to prove stability.

We presented in this paper convergence investigations with respect to numerical integration related to the calculation of the Floquet exponents. An example of misuse of stability analysis is presented as well as a mean to overcome this issue. By interpolating linearly the model matrices forming

the LTP model, and thus up-sampling the data, it was possible to obtain trustful results and thus to conclude on the stability of a time-periodic system. Such a method is foreseen to be particularly adapted to check the stability of time-periodic plants when the controller design is based for simplicity reasons on time-invariant systems.

This approach is however not suited for an analysis in the frequency domain. As Floquet stability analysis is applied to the homogenous part of LTP systems, input/output behavior, as well as damping estimation, cannot be implemented in the view of LTI systems. This constitutes one of the major limitations of the method, and could be for instance perfectly coupled with lifting techniques for the analysis of the LTP models represented by a lifted LTI representation.

## APPENDIX

### Frobenius Norm

The Frobenius matrix norm can be defined for a matrix  $M \in \mathbb{C}^{n \times n}$  composed of elements  $m(i, j)$ , as

$$(7) \quad \|M\|_F = \sqrt{\sum_{i,j} |m(i, j)|^2}$$

### Floquet Theory Overview

We consider the system of order  $n$  for a time  $t \in [0, T]$ . The homogenous differential equation of Eq. (1) can be written:

$$(8) \quad \dot{x}(t) = A(t)x(t)$$

Since the degrees of freedom of a dynamic system at  $t$  must be a linear combination of the state at  $t_0$ , the homogeneous solution can be formulated as

$$(9) \quad x_H(t) = \Phi(t, t_0)x(t_0)$$

where  $\Phi(t, t_0) \in \mathbb{R}^{n \times n}$  corresponds to the state-transition matrix (also called monodromy matrix) relating the state at  $t$  to the state at  $t_0$ . Inserted in Eq. (8), one comes to:

$$(10) \quad \dot{\Phi}(t, t_0) = A(t)\Phi(t, t_0)$$

Teschl [21] demonstrated that the monodromy matrix also has the following properties:

$$(11) \quad \begin{aligned} \Phi(t_2, t_0) &= \Phi(t_2, t_1)\Phi(t_1, t_0) \\ \Phi(t_2, t_1) &= \Phi^{-1}(t_1, t_2) \\ \Phi(t, t) &= I \\ \Phi(t+T, t_0+T) &= \Phi(t, t_0) \end{aligned}$$

Using Eq. (8) and (10), as well as the periodicity of  $A(t)$ , the differential equation for  $\Phi(t, t_0)$

becomes:

$$(12) \quad \frac{d}{dt}(\Phi(t+T, t_0+T)) = \mathbf{A}(t)\Phi(t+T, t_0)$$

and thus proves that  $\Phi(t+T, t_0)$  is also solution of eq. (10). It can therefore be written as a linear combination of  $\Phi(t, t_0)$  using the constant matrix  $\mathbf{K}(t_0) \in \mathbb{R}^{n \times n}$ :

$$(13) \quad \Phi(t+T, t_0) = \mathbf{K}(t_0)\Phi(t, t_0)$$

We now define the constant matrix  $\mathbf{R}(t_0) \in \mathbb{R}^{n \times n}$  and  $\mathbf{P}(t) \in \mathbb{R}^{n \times n}$  such as

$$(14) \quad \begin{aligned} \mathbf{K}(t_0) &= e^{\mathbf{R}(t_0)T} \\ \mathbf{P}(t) &= \Phi(t, t_0)e^{-\mathbf{R}(t_0)t} \end{aligned}$$

Using the properties of Eq. (11), one can prove that

$$(15) \quad \Phi(t, t_0) = \mathbf{P}(t)e^{\mathbf{R}(t-t_0)}\mathbf{P}^{-1}(t_0)$$

and then straightforward that  $\mathbf{P}(t)$  is a complex  $T$ -periodic non-singular matrix. This corresponds to one of the principal results of the Floquet theory.

Using Eq. (13), it follows that

$$(16) \quad \Phi(t+NT, t_0) = \mathbf{K}(t_0)^N \Phi(t, t_0)$$

where  $N$  is an integer counting the number of periods. It clearly illustrates that the information describing the solution is contained in the state-transition matrix over one period. And therefore, only a single period is needed to conclude on the stability of the LTP system.

Let the complex matrix  $\Theta \in \mathbb{R}^{n \times n}$  be the matrix of eigenvalues<sup>\*\*\*</sup> of  $\mathbf{K}(t_0)$ , and  $\Lambda \in \mathbb{R}^{n \times n}$  the matrix of eigenvalues of  $\mathbf{R}(t_0)$ . As both matrices have the same eigenvectors, one can state that:

$$(17) \quad \begin{aligned} &\exists \mathbf{S}(t_0) \in \mathbb{C}^{n \times n} \text{ such that} \\ \left\{ \begin{aligned} \mathbf{K}(t_0) &= \mathbf{S}(t_0) \Theta \mathbf{S}(t_0)^{-1} \\ \mathbf{R}(t_0) &= \mathbf{S}(t_0) \Lambda \mathbf{S}(t_0)^{-1} \\ \mathbf{K}(t_0)^N &= \mathbf{S}(t_0) \Theta^N \mathbf{S}^{-1}(t_0) \\ \mathbf{NR}(t_0) &= \mathbf{S}(t_0) N\Lambda \mathbf{S}^{-1}(t_0) \end{aligned} \right. \end{aligned}$$

which is determinant for conclusions on stability. Using these two properties, a stability criterion can be formulated using either the eigenvalues<sup>\*\*\*</sup>  $(\theta_i)_{i \in \llbracket 1, n \rrbracket}$  of  $\Theta$  or  $(\lambda_i)_{i \in \llbracket 1, n \rrbracket}$  of  $\Lambda$ , as  $\Lambda = 1/T \ln(\Theta)$ :

$$(18) \quad \begin{aligned} &\text{The system} \\ &\text{is asym.} \Leftrightarrow \forall i \in \llbracket 1, n \rrbracket, \left\{ \begin{aligned} &(1) \operatorname{Re}(\lambda_i) < 0 \\ &\text{or respectively} \\ &(2) |\theta_i| < 1 \end{aligned} \right. \\ &\text{stable} \end{aligned}$$

<sup>\*\*\*</sup> We assume the system is non singular.  
<sup>†††</sup> Or also diagonal elements in this case.

This criterion is illustrated in Fig. 20.

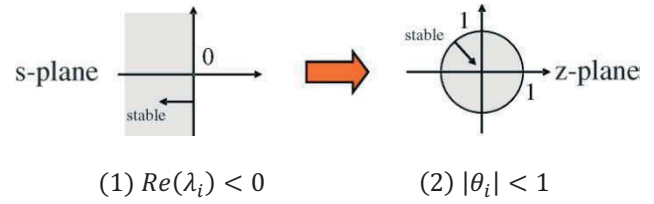


**Fig. 20:** Stability criterion of Floquet exponents and multipliers

In practice, the matrix  $\mathbf{K}(t_0)$  needs to be calculated in order to generate the eigenvalue matrix  $\Theta$  and therefore conclude on the stability of the LTP system. Eq. (13) is valid for all  $t$  and especially for  $t = t_0 = 0$ , hence in this equation:

$$(19) \quad \begin{aligned} \Phi(T, 0) &\stackrel{\text{Eq. (13)}}{=} \mathbf{K}(0) \Phi(0, 0) \\ &\stackrel{\text{Eq. (11)}}{=} \mathbf{K}(0) \end{aligned}$$

The matrix  $\mathbf{K}(0) = \Phi(T, 0)$  can be calculated by integrating  $\dot{\Phi}(t, 0) = \mathbf{A}(t)\Phi(t, 0)$  over one period.

## Runge-Kutta Integration Scheme

### 2<sup>nd</sup> Order

For the computation of the transition matrix, the second-order Runge-Kutta integration scheme to compute the  $i$ -th column of  $\Phi(T, 0)$  can be written as:

$$(20) \quad \begin{aligned} &\forall k \in \llbracket 1, N-1 \rrbracket, \mathbf{x}_{k+1} = \mathbf{x}_k + \frac{\Delta t}{2}(\mathbf{k}_1 + \mathbf{k}_2) \\ &\text{where } \begin{cases} \mathbf{k}_1 = \mathbf{A}_k \mathbf{x}_k \\ \mathbf{k}_2 = \mathbf{A}_{k+1}(\mathbf{x}_k + \Delta t \mathbf{k}_1) \end{cases} \end{aligned}$$

with initial condition  $\mathbf{x}_1^t = \left(0, \dots, 0, \underset{i}{1}, 0, \dots, 0\right)$

### 4th Order

In the case of the fourth-order scheme:

$$(21) \quad \begin{aligned} &\forall k \in \llbracket 1, N-1 \rrbracket, \\ &\mathbf{x}_{k+1} = \mathbf{x}_k + \frac{\Delta t}{2}(\mathbf{k}_1 + 2\mathbf{k}_2 + 2\mathbf{k}_3 + \mathbf{k}_4) \\ &\text{where } \begin{cases} \mathbf{k}_1 = \mathbf{A}_k \mathbf{x}_k \\ \mathbf{k}_2 = \left(\frac{\mathbf{A}_{k+1} + \mathbf{A}_k}{2}\right) \left(\mathbf{x}_k + \frac{\Delta t}{2} \mathbf{k}_1\right) \\ \mathbf{k}_3 = \left(\frac{\mathbf{A}_{k+1} + \mathbf{A}_k}{2}\right) \left(\mathbf{x}_k + \frac{\Delta t}{2} \mathbf{k}_2\right) \\ \mathbf{k}_4 = \mathbf{A}_{k+1}(\mathbf{x}_k + \Delta t \mathbf{k}_3) \end{cases} \\ &\text{with initial condition } \mathbf{x}_1^t = \left(0, \dots, 0, \underset{i}{1}, 0, \dots, 0\right) \end{aligned}$$

## REFERENCES

- [1] Johnson, W., "A Comprehensive Analytical Model of Rotorcraft Aerodynamics and Dynamics", Theory Manual, Johnson Aeronautics, 1996.
- [2] Polychroniadis, M., Achache, M., "Higher harmonic control: Flight tests of an experimental system on SA349 research gazelle", 42<sup>nd</sup> AHS annual forum, Washington D.C, 1986.
- [3] Wood, E.R., Powers, R.W., Cline, J.H., Hammond, C.E., "On developing and flight testing a higher harmonic control system", 39<sup>th</sup> AHS annual forum, St. Louis, Missouri, 1983.
- [4] Roth, D., Enekl, B., Dieterich, O., "Active Rotor Control by Flaps for Vibration Reduction, full scale demonstrator and first flight test results", 32<sup>nd</sup> European Rotorcraft Forum, Maastricht, the Netherlands, September 12 – 14 2006.
- [5] Dieterich, O., Enekl, B., Roth, D., "Trailing edge flaps for active rotor control – aeroelastic characteristics of the ADASYS rotor system", 62<sup>nd</sup> AHS annual forum, Phoenix, AZ, 2006.
- [6] Straub, F.K., Anand, V.R., Birchette, T.S., Lau, B.H., "Wind tunnel test of the SMART active flap rotor", 65<sup>th</sup> AHS annual forum, Grapevine, TX, 2009.
- [7] Dieterich, O., Konstanzer, P., Roth, D., Ayadi, W., Reber, D., Well, K.H., *Model based H<sub>∞</sub> control for helicopter vibration reduction – flight tests with active trailing edge flaps*, 33<sup>rd</sup> European rotorcraft forum, Kazan, RU, 2007.
- [8] Konstanzer, P., "Decentralized Vibration Control for Active Helicopter Rotor Blades", Fortschritt-Berichte VDI, Reihe 8, Nr. 923, VDI Verlag Düsseldorf, Germany, 2002.
- [9] Bebesel, M., Schoell, E., Polz, G., "Aerodynamic and aeroacoustic layout of the ATR (Advanced Technology Rotor)", 55<sup>th</sup> AHS annual forum, Montreal, Canada, 1999.
- [10] Johnson, W., "Technology drivers in the development of CAMRAD II", AHS Aeromechanics Specialists Conference, San Francisco, California, 1994.
- [11] Hohenhemser, K. H., Yin, S. H., "Some Applications of the Method of Multiblade Coordinates", Journal of the American Helicopter Society, 1972.
- [12] Floquet, G., "Sur les Équations Différentielles Linéaires", Annales de l'École Normale Supérieure, Paris, December 1883.
- [13] Mohler, R.R., "Nonlinear systems, Dynamics and Control", vol. 1, Prentice-Hall, Inc., 1991.
- [14] Johnson, W., "Helicopter Theory", Dover Publications, inc., 1980.
- [15] Peters, D. A., "Fast Floquet Theory and Trim for Multi-bladed Rotorcraft", 51<sup>st</sup> AHS annual forum, Fort Worth, TX, May 9-11, 1995.
- [16] Peters, D. A., Lieb, S. M., "Significance of Floquet Eigenvalues and Eigenvectors for the Dynamics of Time-Varying Systems", submitted to the AHS International 65<sup>th</sup> Annual National Forum & Technology Display, Grapevine, Texas, May 27-29, 2009.
- [17] Subramanian, S., Gaonkar, G. H., "Parallel Fast Floquet Analysis of Trim and Stability for Large Helicopter Models", 22<sup>nd</sup> European Rotorcraft Forum and 13<sup>th</sup> European Helicopter Association Symposium, Brighton, UK, Sept. 16-19, 1996.
- [18] Venkataratnam, S., Subramanian, S. and Gaonkar, G. H., "Fast-Floquet Analysis of Helicopter Trim and Stability with Distributed and Massively Parallel Computing", 23<sup>rd</sup> European Rotorcraft Forum, Dresden, Germany, Sept. 16-18, 1997.
- [19] Wang, X., Hale, J. K., "On monodromy matrix computation", Tech. Report IPST Technical Paper Series Number 756, Institute of Paper Science and Technology, Atlanta, Georgia, October 1998.
- [20] Van der Kloet, P., Neerhoff, F., "Floquet numbers and dynamic eigenvalues", accepted for publ. ProRisc, 2003.
- [21] Teschl, G., "Ordinary Differential Equations and Dynamical Systems", Faculty for Mathematics, Nordbergstraße 15, Universität Wien, 1090 Wien, Austria.